



# Evaluation of the long-term effect of lime treatment on a silty soil embankment after seven years of atmospheric exposure: Mechanical, physicochemical, and microstructural studies

Geetanjali Das, Andry Razakamanantsoa, Gontran Herrier, Lucile Saussaye, Didier Lesueur, Dimitri Deneele

## ► To cite this version:

Geetanjali Das, Andry Razakamanantsoa, Gontran Herrier, Lucile Saussaye, Didier Lesueur, et al.. Evaluation of the long-term effect of lime treatment on a silty soil embankment after seven years of atmospheric exposure: Mechanical, physicochemical, and microstructural studies. Engineering Geology, 2021, 281, pp.105986. 10.1016/j.enggeo.2020.105986 . hal-03169747

**HAL Id: hal-03169747**

**<https://hal.science/hal-03169747v1>**

Submitted on 3 Feb 2023

**HAL** is a multi-disciplinary open access archive for the deposit and dissemination of scientific research documents, whether they are published or not. The documents may come from teaching and research institutions in France or abroad, or from public or private research centers.

L'archive ouverte pluridisciplinaire **HAL**, est destinée au dépôt et à la diffusion de documents scientifiques de niveau recherche, publiés ou non, émanant des établissements d'enseignement et de recherche français ou étrangers, des laboratoires publics ou privés.



Distributed under a Creative Commons Attribution - NonCommercial 4.0 International License

# Evaluation of the long-term effect of lime treatment on a silty soil embankment after seven years of atmospheric exposure: mechanical, physicochemical, and microstructural studies

Geetanjali Das<sup>a,\*</sup>, Andry Razakamanantsoa<sup>a</sup>, Gontran Herrier<sup>b</sup>, Lucile Saussaye<sup>c</sup>, Didier Lesueur<sup>d</sup>, Dimitri Deneele<sup>a,c</sup>

<sup>a</sup>*GERS, Université Gustave Eiffel, IFSTTAR, F-44344 Bouguenais, France*

<sup>b</sup>*Lhoist Recherche et Développement, rue de l'Industrie 31, 1400 Nivelles, Belgique*

<sup>c</sup>*CEREMA Blois, France*

<sup>d</sup>*Lhoist Southern Europe, 15 rue Henri Dagallier, 30040 Grenoble, France*

<sup>e</sup>*Institut des Matériaux Jean Rouxel de Nantes, Université de Nantes, CNRS, 2 chemin de la Houssinière, BP 32229, 44322 Nantes Cedex 3, France*

## Abstract

The long-term effect of lime treatment was evaluated on a 2.5 % lime-treated experimental embankment after seven years of atmospheric exposure. The evaluation was done by comparison of (i) the mechanical performance of the field sampled specimens with laboratory cured specimens, and (ii) the physicochemical and microstructural properties of the samples from the lime-treated embankment with specimens obtained from an untreated embankment constructed near to it as a reference embankment.

An average Unconfined Compressive Strength (UCS) level of 3.29 MPa was measured in the lime-treated specimens sampled from the core of the embankment. This UCS level was found to be comparable to the UCS of accelerated-cured specimens obtained at a laboratory scale. Thus, such levels of UCS can be expected after long-term in-situ curing. Scanning electron microscope images evidenced the contribution of the formation of cementitious bonding towards such UCS evolution in the lime-treated specimen. The persistence of the lime effect within the core of the embankment was confirmed by the presence of a pH greater than 11. However, a relative decrease in the pH and water content was observed in the upper layer compared to the core of the lime-treated embankment. This indicates that the effect of lime was lost in the upper layer under constant soil-atmosphere interaction and due to the development of vegetation roots. Pore structure observations made by Mercury Intrusion Porosimetry (MIP) and Barrett-Joiner-Halendapore (BJH) methods highlight the formation of smaller pores (diameter < 3000 Å) under lime effect. These smaller pores have contributed towards the evolution of suction in the core-sampled specimens of the lime-treated embankment. This has led to the long-term water retention capacity of the lime-treated soil. BJH was able to detect mesopore-formation (25-500 Å) under the lime effect in a more precise manner compared to MIP. The evolution of mesopores was found to be coincident with the development of strength and specific surface area of the lime-treated soil.

**Keywords:** *lime treatment; compressive strength; embankment; mesopores; atmospheric exposure.*

## 1. Introduction

Management of natural resources is a critical challenge in any land development project, especially for projects related to earthworks. A cost-effective way to conserve natural resources is to use soil located directly in the land reserved for the project. This makes it essential to improve the engineering properties of the available soil. In this regard, soil improvement by lime is known to be an efficient and economical technique that leads to improved bearing capacity, strength, modulus, etc. (Al-Mukhtar et al., 2012; Bell, 1996; Diamond and Kinter, 1965; Little, 1995; Osula, 1996). Additionally, the lime-treated soil structure is also known to be eco-friendly as the material can be entirely reused after the deconstruction of the structure (Hopkins et al., 2007).

Most studies conducted on soil improvement by lime treatment were obtained from laboratory test results (Ali and Mohamed, 2019; Lemaire et al., 2013; Verbrugge et al., 2011) while the feedback from field performance is less investigated. It is worth noting that the conditions faced by the lime-treated soil under the laboratory- and field-testing environments are relatively different.

Several studies have reported long-term strength improvement in pavement layers stabilized with lime (Aufmuth, 1970; Cardoso and das Neves, 2012; Little, 1995; McDonald, 1969). Aufmuth (1970) concluded that the in-situ California Bearing Ratio (CBR) value observed in lime stabilized pavement layers significantly rises with age and tends to appear permanent if compared to the CBR value of the same soil without stabilization. McDonald (1969) confirmed the effectiveness of lime treatment through a study made on pavements subjected to low, medium, and heavy traffics flow after about 13 years from construction. This was in terms of improved smoothness or rideability and better structural response as indicated by deflection measurements. Cardoso and Neves (2012) demonstrated the effectiveness of lime in reducing the overall settlement rate of an embankment built with marls. They showed how lime treatment induced a decrease in the secondary consolidation of the marls with increased curing, reduced the swelling potential, and increased its stiffness.

So far, few studies have reported the behaviour of lime-treated specimens sampled from real or experimental earth structures submitted to long-term environmental exposure. Rosone et al. (2018) studied the effect of seasonal wetting and drying cycles for over 18 months on specimens obtained from lime-treated expansive clay soil embankment. The suction value measured at the top layer of the embankment was reported to be three times higher than that measured at 0.45 m depth from the surface. Below 0.45 m, the total suction value stabilized at about 1.40 MPa. The high value of suction measured on the top of the embankment was attributed to evapotranspiration, leading to water loss, a rise of suction, and crack development.

Bicalho et al. (2018) described a similar observation with respect to the rise in suction and water content loss in specimens sampled up to a depth of 0.75 m from the surface of a 2 % lime-treated silty clay experimental embankment due to climatic variation. However, with increased curing time, this impact of seasonal variation in the variability of water content and soil suction was minimised, thus indicating the good stability of the lime-treated soil.

The Friant-Kern Canal construction in California, United States, was based on 4 % quicklime by weight to stabilize a highly plastic clay soil in permanent contact with water (Herrier et al., 2012; Knodel, 1987). More than 40 years after construction, the study evidenced the increased long-term strength, reduction in swelling and shrinkage potential, as well as significant resistance to erosion, thus showing the improved geo-mechanical stability of the structure (Akula et al., 2020).

All these studies have demonstrated the effectiveness of lime treatment over time and, to an extent, the effect of the soil atmosphere interaction on the modification of properties of lime-treated soil. Beyond the general behaviour mentioned herein, more investigation is needed with respect to strength and microstructural modifications induced by long-term lime treatment on structures cured in the open atmosphere.

The purpose of this study was to thoroughly evaluate the influence of lime treatment in an atmospherically cured lime-treated embankment after seven years of exposure to wet environmental

conditions. The climatic condition of the construction region can be referred to in Makki-Szymkiewicz et al. (2015), who investigated the embankment at an early age (up to 1 year from construction) to assess its hydraulic performance. They demonstrated that if proper mixing and compaction process is maintained during construction, a permeability of  $10^{-9}$  m/s can be obtained, which was similar to the untreated soil. The present study demonstrates an extended investigation regarding the effectiveness of lime treatment in the long-term. The examination of the lime-treated structure was made in terms of strength, physicochemical characteristics, and microstructure, which was lacking in the studies reported above.

The first part of the study focuses on (i) evaluating the UCS of the lime-treated soil, (ii) examining the presence of cementitious bonding within the fabric of the lime-treated soil, and (iii) investigating the long-term effect of lime treatment on water content, suction, and pH. The second part presents the effect of lime treatment on pore structure and specific surface area modifications.

## 2. Studied embankment, samples, and methods

### 2.1. Materials and implementation of the embankment

The soil used is a silty soil from Marche-Les-Dames (MLD), Belgium, with the following mineralogy: Illite, Kaolinite, and Chlorite as clay minerals along with Quartz and Feldspars. All information about the embankment construction can be obtained from Makki-Szymkiewicz et al. (2015).

The lime-treated embankment was built with 2.5 % of quicklime (CaO), a Proviacal ® DD CL 90-Q supplied by Lhoist. For reference purposes, an untreated embankment was constructed under the same conditions. The maximum dry densities,  $\rho_{d \max}$  of the untreated and 2.5 % lime-treated soil obtained by Standard Proctor test (as per ASTM D698-12e2) were 18.2 kN/m<sup>3</sup> and 17.3 kN/m<sup>3</sup>, respectively, and the Optimum Moisture Contents (OMCs) were 14.6 % and 17.8 %, respectively. Both embankments were compacted by a vibratory sheep foot roller at a moisture content of about 1.1 times of optimum. The lime-treated and the untreated embankment were compacted in 6 and 3 layers, respectively. The average water content recorded after completion of compaction of the untreated and the lime-treated embankment was 17.0 % and 19.4 %, respectively.

### 2.2. Specimens sampling from the embankment and sample preparation for laboratory test

During deconstruction, at first, few specimens were gathered at different depths from the surface up to a depth of 0.12 m (i.e., in the regions close to the surface) to understand the impact of seasonal variation and vegetation roots in the lime-treated embankment. Then the soil near the surface was removed to limit the effect of weathering and plant roots. Later, trenches were excavated (Fig. 1) for sampling soil specimens at different depths throughout the core of the embankment.

A single trench was made on the untreated embankment (Fig. 2). Four trenches were excavated across the lime-treated embankment: T1 and T2 located towards the South-West, and T3 and T4 were located towards the North-East (Fig. 3). Specimens were collected throughout the trenches described in Fig. 2 and Fig. 3 for the untreated and lime-treated embankments, respectively.

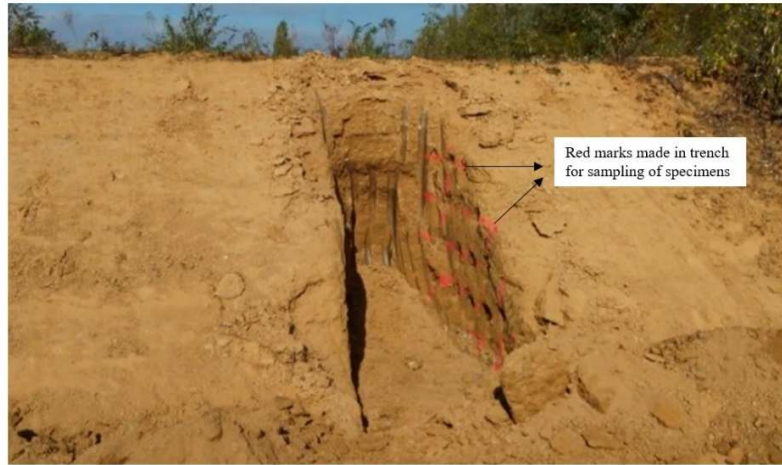


**Fig. 1:** Trench excavated in the lime-treated embankment (T2) for the sampling of specimens

The following nomenclature is used here to identify the various specimens. The specimens collected from the trench excavated in the untreated embankment are referred to as 'Nat', followed by the number displayed in the cross-section (Fig. 2). Similarly, specimens collected from the trench of the lime-treated embankment are referred to as 'T1', 'T2', 'T3', and 'T4', followed by the number in the corresponding cross-section (Fig. 3).

The trenching of the untreated embankment was relatively easy to perform, as the compacted soil was damp and less cohesive. However, block-cutting was not possible due to the low cohesion of the soil.

In the lime-treated embankment, two types of sampling were carried out. A compacted cubic block of about  $0.40 \text{ m}^3$  volume was cut from trenches using an excavator. It is worth noting that the process of block sampling was particularly complicated due to the rigidity of the soil. The second type of sampling consists of recovering smaller samples taken from each point of sample collection of the four trenches (Fig. 3). All specimens sampled were packed in a sealed bag and transported to the laboratory with care.

For strength measurement, two compacted cubic blocks were sampled from point T1-1 and T2-4, located at a depth of 0.30 m and 0.75 m normal to the slope, respectively (Fig. 3). These blocks were later trimmed at the laboratory to obtain specimens having dimensions of length ( $l$ ) and diameter ( $d$ ) with an  $l/d$  ratio of 2 and 1. The ' $l$ ' and ' $d$ ' of specimens corresponding to  $l/d$  ratio of 2 were 0.08 m and 0.04 m, respectively, and while it was 0.05 m for both ' $l$ ' and ' $d$ ' for specimens corresponding to  $l/d$  ratio of 1. Samples of dimension  $l/d = 2$  were obtained as ASTM D 2166 (ASTM, 2006) recommends the standard size of specimens to be within  $l/d$  ratio of 2 and 2.5 for the UCS test. Additional samples of  $l/d = 1$  were trimmed.

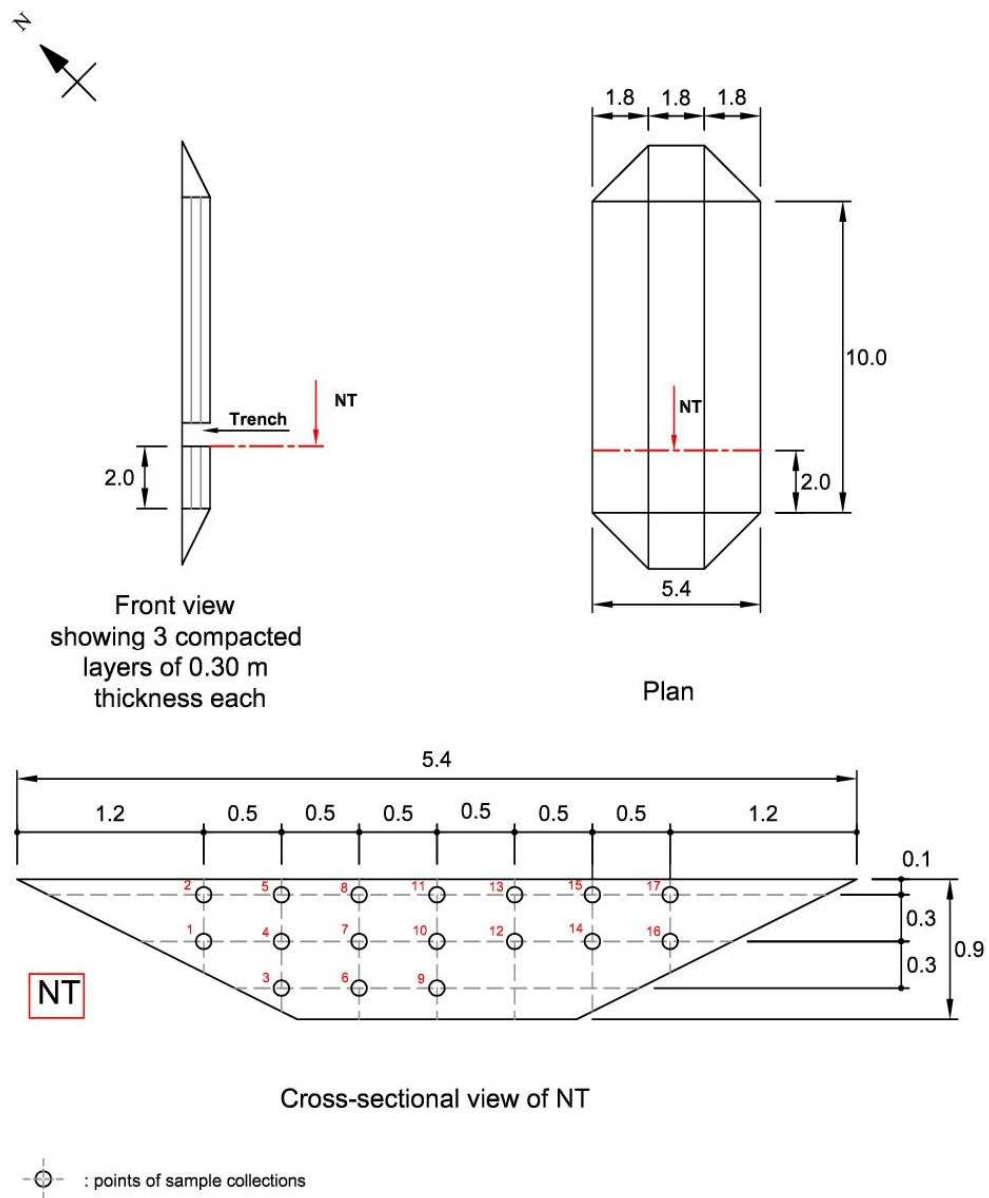


**Fig. 2:** Plan view, Front view along with Cross-sectional view of the excavated trench made for sample collections from the Untreated embankment (All units in meter)

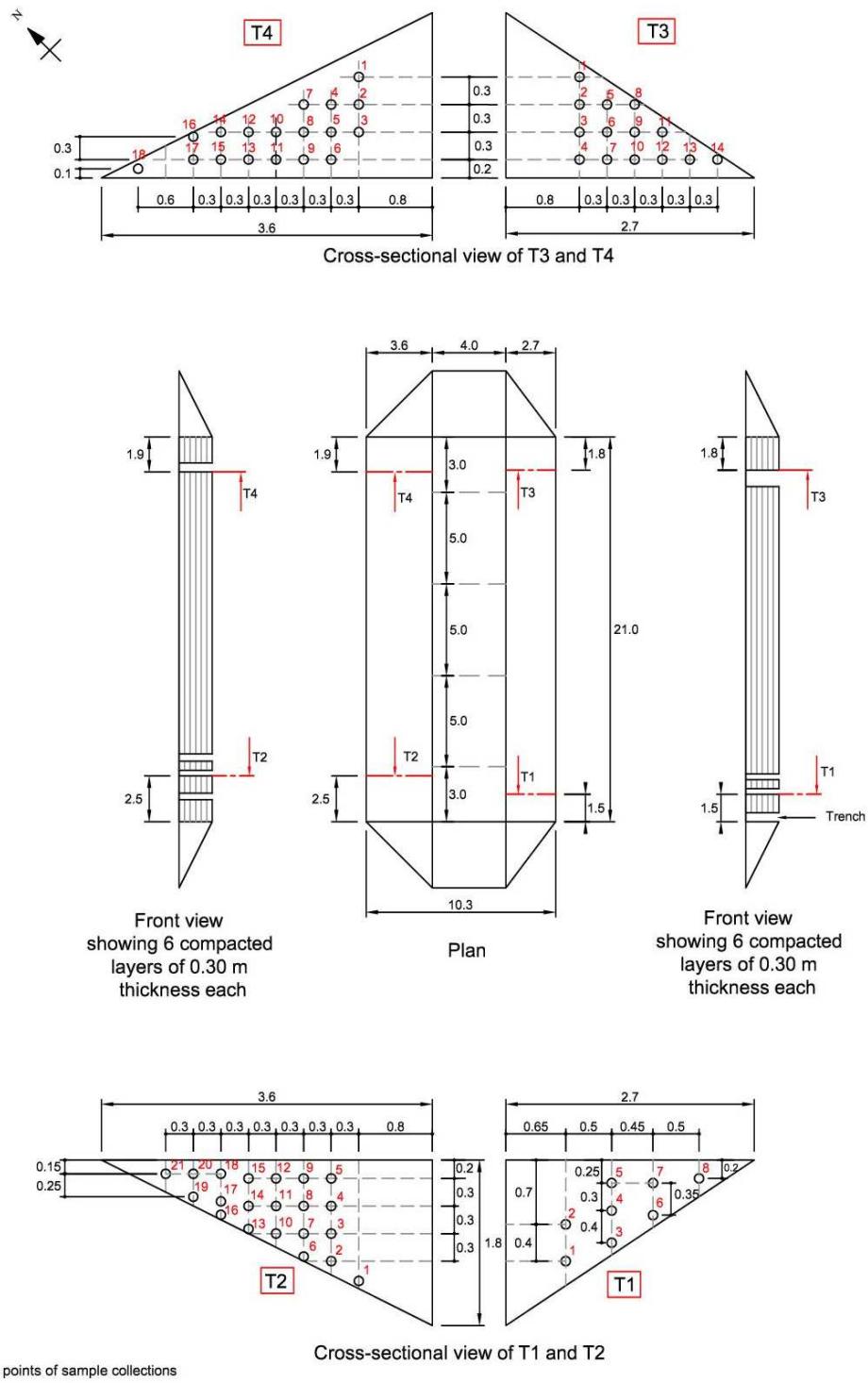


**Fig. 3:** Plan view, Front view along with Cross-sectional view of the excavated trenches made for sample collections from the lime-treated embankment (*All units in meter*)

### 2.3. Laboratory tests

The UCS of the samples was measured using a mechanical press with a load sensor of 25 kN capacity. Measurements were performed at a constant deformation rate of 1 mm/min.

The soil fabric was assessed using a Scanning Electron Microscope (SEM) observation. The high-field emission Hitachi SU5000 SEM device was used for this purpose.

The physicochemical behaviour was investigated by measuring the water content, suction, and pH of the collected samples. Specimens sampled throughout the core of the trenches (Figs. 2 & 3) were subjected to all three tests. At the same time, the upper-layer-sampled specimens were subjected to water content and pH measurements. The water content measurement was carried out by oven drying at 105°C (ASTM, 2010), and the suction measurements were conducted using the WP4C Dewpoint Potentiometer (Decagon device). The pH measurement was executed by HI 2210 pH Meter. Samples collected were sieved through a 2 mm mesh size and then suspended in distilled water in a liquid-solid ratio of 5:1 (volume fraction) for 1 hour. The pH of the suspended solution was then recorded.

The Specific Surface Area (SSA) of compacted freeze-dried samples were analysed by Brunauer–Emmett–Teller (BET) (Brunauer et al., 1938) test using Micromeritics TriStar II PLUS. Since SSA values were measured in compacted specimens, hence the measured values can be possibly lower than those of powdered samples under similar conditions.

Pore characterization was done on compacted freeze-dried samples using MIP test and BJH method. MIP test was conducted using Micromeritics Auto Pore IV, while the BJH method analysed the pore structure from the data obtained by the BET test. The observed pore structure was classified based on the International Union of Pure and Applied Chemistry (IUPAC) (Rouquerol et al., 1994), which categorizes the pore-width as macropores ( $> 500 \text{ \AA}$ ), mesopores ( $20\text{--}500 \text{ \AA}$ ), and micropores ( $< 20 \text{ \AA}$ ). Lime treatment was shown to generate the development of smaller pores of diameter less than  $3000 \text{ \AA}$  (Bhuvaneshwari et al., 2014; Cuisinier et al., 2011). This smaller pore includes a part of the macropores range and the total range of mesopores and micropores as per IUPAC classification. Thus, to obtain a more accurate description of the size of pore evolution, this study uses both the MIP test and the BJH method. In this study, the analysis of Pore Size Distribution (PSD) by BJH was made considering the desorption branch of the isotherm because the formation of the cylindrical meniscus is assumed to be stable in the desorption branch as reported by Bin et al. (2007) and Cai and Hu, (2019). The contribution of lime treatment on pore structure modification was investigated by a comparative analysis of pore characterizations made on four selected samples. These specimens were collected at two constant depths to avoid any possible additional stress impact: untreated specimens Nat 1, Nat 2, and lime-treated specimens T2-2, T2-3. Specimens Nat 1 and T2-2 were sampled at 0.15 m depth, whereas Nat 2 and T2-3 are located at 0.45 m depth, normal to the slope (Figs. 2 & 3).

The distribution of moisture content, pH, and SSA of the specimens sampled from the core of the embankments are presented using contour plots obtained by using the mapping software: Surfer 13.

Table 1 summarizes the complete testing programs with the corresponding identifications and numbers of specimens.

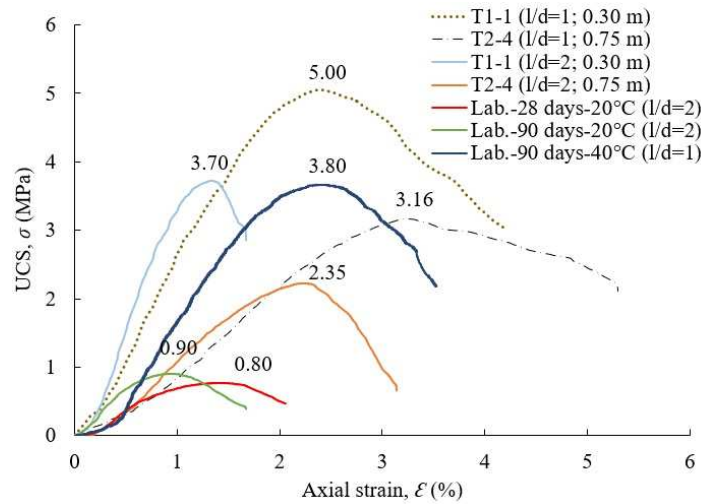
**Table 1:**

Test programs with samples identifications and numbers

| Sample type                             | Test name              | No. of samples | Sample name   |
|---|------------------------|----------------|---|
| Laboratory (Lab.) specimens             | UCS                    | 3              | Lab.-28days-20°C (l/d=2), Lab.-90days-20°C (l/d=2),<br>Lab.-90days-40°C (l/d=1)   |
| In-situ (upper layer-sampled) specimens | Water content, pH      | 13 each        | T1 and T2   |
|   | UCS                    | 4              | T1-1 (l/d=2 ; 0.30 m), T2-4 (l/d=2 ; 0.75 m),<br>T1-1 (l/d=1 ; 0.30 m), T2-4 (l/d=1 ; 0.75 m)   |
|   | SEM                    | 2              | Nat 2 (0.45 m), T1-1 (0.30 m)   |
|   | Water content, pH, SSA | 78 each        | All specimens shown in cross-sections of Fig. 2 & 3   |
| In-situ (core-sampled) specimens        | PSD by MIP             | 4              | Nat 1 (0.15 m), Nat 2 (0.45 m),<br>T2-2 (0.15 m), T2-3 (0.45 m)   |
|   | PSD by BJH             | 17             | Nat 1 (0.15 m), Nat 2 (0.45 m), T1-1 (0.30 m),<br>T2-2 (0.15 m), T2-3 (0.45 m), T2-4 (0.75 m),<br>T1-2, T1-3, T1-6, T1-7, T2-13, T3-7, T3-9,<br>T3-14, T4-8, T4-11, T4-12 |

### 3. Results

#### 3.1. Unconfined Compressive Strength

**Fig. 4:** UCS measured from the field- and laboratory-cured specimens

The UCS values of the four trimmed core-sampled specimens from T1-1 (0.30 m) and T2-4 (0.75 m), as mentioned in section 2.2, are presented in Fig. 4. Specimens from T1-1 show UCS values of 3.70 MPa (l/d = 2) and 5.00 MPa (l/d = 1). Specimens from T2-4 show UCS values of 2.35 MPa (l/d = 2) and 3.16 MPa (l/d = 1). The corresponding water content of these specimens during the UCS test was measured to be around 11.0 %.

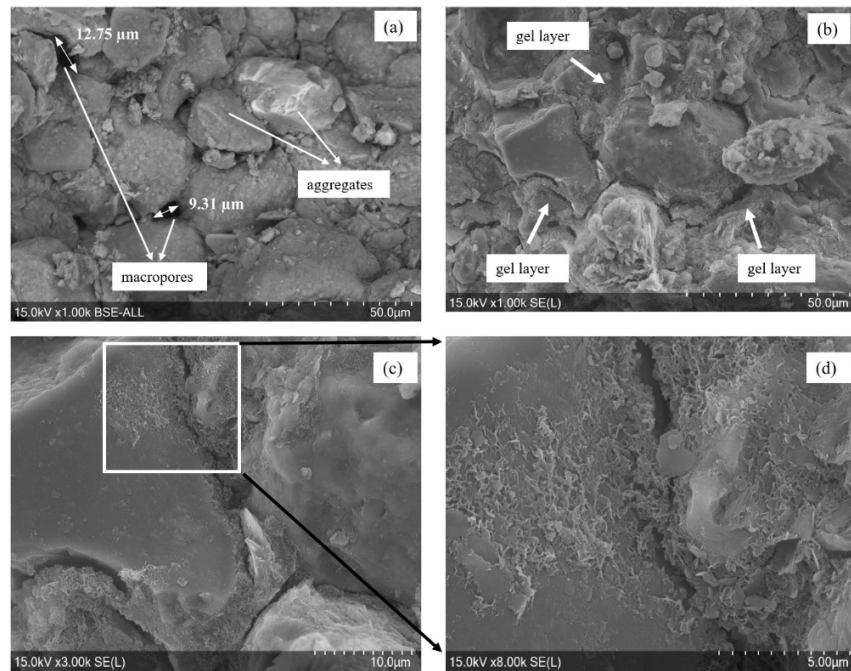
The UCS measured in the in-situ specimens was compared with three laboratory-cured samples prepared with similar soil and the same lime content and water content as the field specimens. Two laboratory compacted specimens of dimension having l/d ratio of 2 were cured for 28- and 90-days at 20°C. The 28-day curing was considered as a reference short curing period, whereas 90-day was the long curing period at a laboratory scale. Since no laboratory study was made with specimens subjected to 7 years of curing, a third laboratory compacted sample was subjected to accelerated curing (at 40°C) for 90 days. Lemaire et al. 2013 and Zhang et al. 2020 have demonstrated that the increase in temperature accelerates the soil-water-lime chemical reactions resulting in a rapid rise of UCS level in the lime-treated soil.

Fig. 4 shows that the UCS measured for 28- and 90-days laboratory cured specimens at 20°C (of dimension l/d = 2) were 0.80 and 0.90 MPa, respectively. While the UCS measured for the accelerated cured specimens (of size l/d = 1) was 3.80 MPa.

### 3.2. SEM observations

Fig. 5 presents the SEM images showing the fabric structures of Nat 2 (untreated specimen sampled at 0.45 m depth from the slope) and T1-1 (lime-treated specimen sampled at 0.30 m depth from the slope) freeze-dried and gold-coated specimens. At a magnification of 1.00k, macropores and aggregates were observed in Nat 2 (Fig. 5 (a)), while in T1-1, the aggregates, minerals, and pores were found to be covered by a gel layer (Fig. 5 (b)).

At higher magnifications (Fig. 5(c & d)), the cementitious bonding was observed between minerals and soil aggregates in T1-1, which is as reported in prior literature (di Sante, 2019; Jha and Sivapullaiah, 2019; Lemaire et al., 2013).



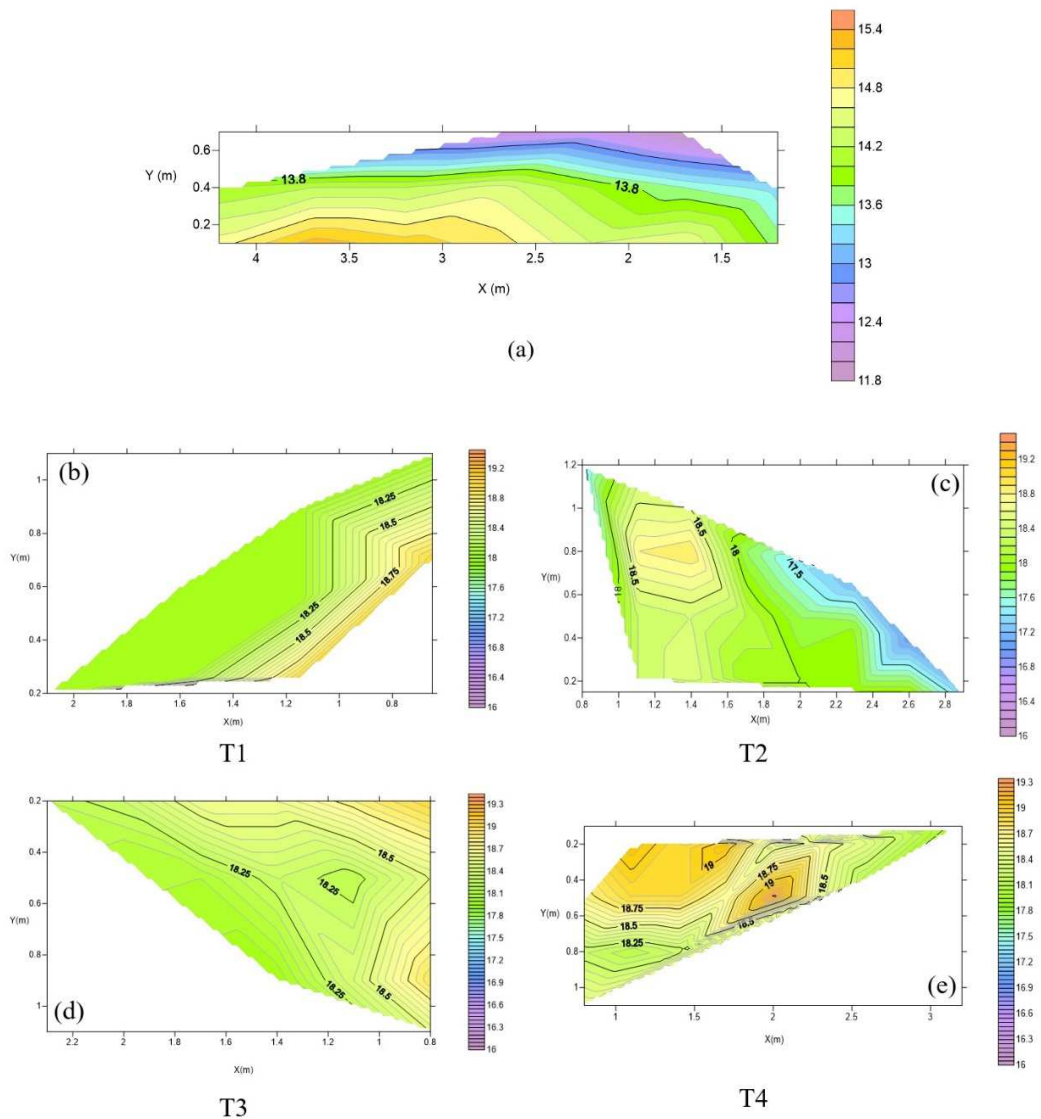
**Fig. 5:** SEM images of specimens Nat 2 (0.45 m) (a) and T1-1 (0.30 m) (b-d) at different magnifications sampled from the core of the embankments

### 3.3. Physicochemical properties

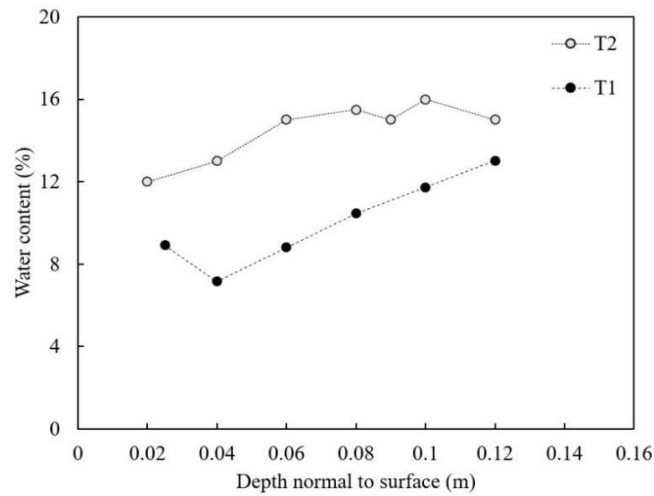
#### 3.3.1. Distribution of water content

Fig. 6 presents the distribution of water content throughout the core of the untreated and lime-treated embankments measured during deconstruction.

In the core of the untreated embankment, the water content was measured to be minimum at the surface, i.e., 11.8 %, and it gradually increased with depths reaching 15.4 % at the subgrade (Fig. 6(a)). While throughout the core of the lime-treated embankment, the water content measured was observed to be unevenly distributed in the range 17-19.3 % (Fig. 6 (b-e)).



**Fig. 6:** Contour plots showing the distributions of water content (%) in the untreated (a) and the cross-sections T1 (b), T2 (c), T3 (d), and T4 (e) of the lime-treated embankments measured during deconstruction



**Fig. 7:** Water content (%) measured on specimens sampled from the upper layer of the lime-treated embankment during deconstruction

Fig. 7 presents the water content measured on the upper layer-sampled specimens of the lime-treated embankment from the cross-sections T1 and T2 up to a depth of 0.12 m normal to the surface. The minimum water content observed in T1 was 7.0 %, while it was 12.0 % for T2. The water content then gradually increased with depth from the surface and reached a maximum value of 15 % for T2 and 13 % for T1.

### 3.3.2. Measurement of suction

The suction measured for all the untreated and the lime-treated core-sampled specimens is presented in Table 2. Due to the presence of 78 samples, measurement of suction was done sequentially, one after the other. This led to a slight variation between the water content measured during suction measurement and the one measured during deconstruction, as seen in Table 2. The suction range measured for the untreated specimens was 0.19-1.14 MPa, which corresponds to a water content range of 9.89-11.71 %. While for the lime-treated soil, the suction range measured was 0.17-2.71 MPa, corresponding to a water content range of 15.8-17.9 % (Table 2).

309

310

311

**Table 2:**

Suction measured on untreated and lime-treated core-sampled specimens

| Sample    | Numbers                     | 1    | 2    | 3    | 4    | 5    | 6    | 7    | 8    | 9    | 10   | 11   | 12   | 13   | 14   | 15   | 16   | 17   | 18   | 19   | 20   | 21   |
|-----------|-----------------------------|------|------|------|------|------|------|------|------|------|------|------|------|------|------|------|------|------|------|------|------|------|
| Untreated | WC (DC) <sup>1</sup><br>(%) | 13.3 | 13.7 | 11.9 | 13.6 | 14.6 | 12.4 | 14.0 | 14.4 | 12.2 | 14.5 | 14.9 | 14.2 | 15.1 | 14.2 | 15.3 | 14.0 | 14.7 |      |      |      |      |
|           | WC (SM) <sup>2</sup><br>(%) | 9.89 | 11.2 | 9.73 | 10.8 | 12.9 | 9.71 | 11.9 | 11.6 | 9.38 | 11.7 | 11.4 | 12.7 | 12.6 | 12.3 | 12.3 | 11.5 | 12.1 |      |      |      |      |
|           | Suction<br>(MPa)            | 1.14 | 0.73 | 0.60 | 0.88 | 0.40 | 0.80 | 0.57 | 0.65 | 1.01 | 0.19 | 0.46 | 0.21 | 0.61 | 0.45 | 0.66 | 0.39 | 0.31 |      |      |      |      |
| T1        | WC (DC)<br>(%)              | 18.2 | 19.0 | 18.1 | 18.2 | 18.7 | 17.9 | 18.2 | 18.2 |      |      |      |      |      |      |      |      |      |      |      |      |      |
|           | WC (SM)<br>(%)              | 17.0 | 18.0 | 17.0 | 17.0 | 18.0 | 16.3 | 17.3 | 17.2 |      |      |      |      |      |      |      |      |      |      |      |      |      |
|           | Suction<br>(MPa)            | 1.15 | 0.80 | 1.29 | 0.76 | 0.72 | 1.47 | 0.78 | 0.71 |      |      |      |      |      |      |      |      |      |      |      |      |      |
| T2        | WC (DC)<br>(%)              | 17.4 | 18.4 | 18.8 | 18.3 | 18.3 | 18.5 | 18.9 | 18.4 | 18.5 | 17.8 | 18.2 | 18.0 | 17.4 | 17.8 | 18.0 | 17.2 | 17.9 | 18.0 | 18.0 | 17.0 | 17.3 |
|           | WC (SM)<br>(%)              | 14.1 | 16.0 | 15.2 | 16.2 | 18.2 | 16.4 | 15.2 | 16.3 | 17.2 | 17.0 | 16.0 | 15.4 | 16.4 | 17.0 | 17.5 | 16.8 | 16.4 | 16.6 | 16.3 | 16.0 | 16.4 |
|           | Suction<br>(MPa)            | 1.51 | 0.86 | 0.89 | 0.34 | 0.40 | 0.55 | 0.95 | 0.83 | 0.93 | 0.80 | 1.29 | 1.75 | 1.10 | 0.83 | 0.80 | 1.27 | 1.29 | 1.03 | 1.39 | 1.61 | 1.13 |
| T3        | WC (DC)<br>(%)              | 18.5 | 18.9 | 18.5 | 19.0 | 18.4 | 18.2 | 18.8 | 18.0 | 18.3 | 18.6 | 18.1 | 18.6 | 18.3 | 18.2 |      |      |      |      |      |      |      |
|           | WC (SM)<br>(%)              | 17.9 | 17.6 | 17.2 | 17.7 | 18.2 | 18.1 | 17.9 | 17.2 | 17.1 | 18.2 | 17.8 | 17.9 | 18.2 | 17.2 |      |      |      |      |      |      |      |
|           | Suction<br>(MPa)            | 0.42 | 0.63 | 0.51 | 0.71 | 0.56 | 0.41 | 0.53 | 0.71 | 0.68 | 0.18 | 0.40 | 0.17 | 0.35 | 0.85 |      |      |      |      |      |      |      |
| T4        | WC (DC)<br>(%)              | 18.5 | 18.2 | 18.7 | 18.1 | 18.9 | 19.1 | 18.2 | 18.9 | 18.9 | 18.6 | 19.1 | 19.3 | 18.4 | 18.5 | 18.6 | 18.1 | 18.4 | 17.9 |      |      |      |
|           | WC (SM)<br>(%)              | 17.9 | 14.5 | 18.0 | 17.3 | 17.6 | 16.6 | 16.9 | 17.1 | 15.3 | 16.5 | 16.6 | 18.5 | 14.5 | 15.8 | 17.2 | 16.1 | 17.5 | 16.9 |      |      |      |
|           | Suction<br>(MPa)            | 0.97 | 0.30 | 0.50 | 0.95 | 0.87 | 1.14 | 0.90 | 1.31 | 1.40 | 1.77 | 1.46 | 0.70 | 2.04 | 2.71 | 1.03 | 1.76 | 0.98 | 1.63 |      |      |      |

<sup>1</sup>WC(DC): Water content measured during the deconstruction of embankments<sup>2</sup>WC(SM): Water content measured during the suction measurement

312

313

314

315

### 3.3.3. Distribution of pH

Fig. 8 presents the distribution of pH throughout the core of the untreated and the lime-treated embankments measured during deconstruction.

The pH value of the untreated embankment was between 8.3 to 8.8 (Fig. 8 (a)). In the lime-treated embankment, the measured pH value ranges between 11.08 and 11.66 (Fig. 8 (b-e)).

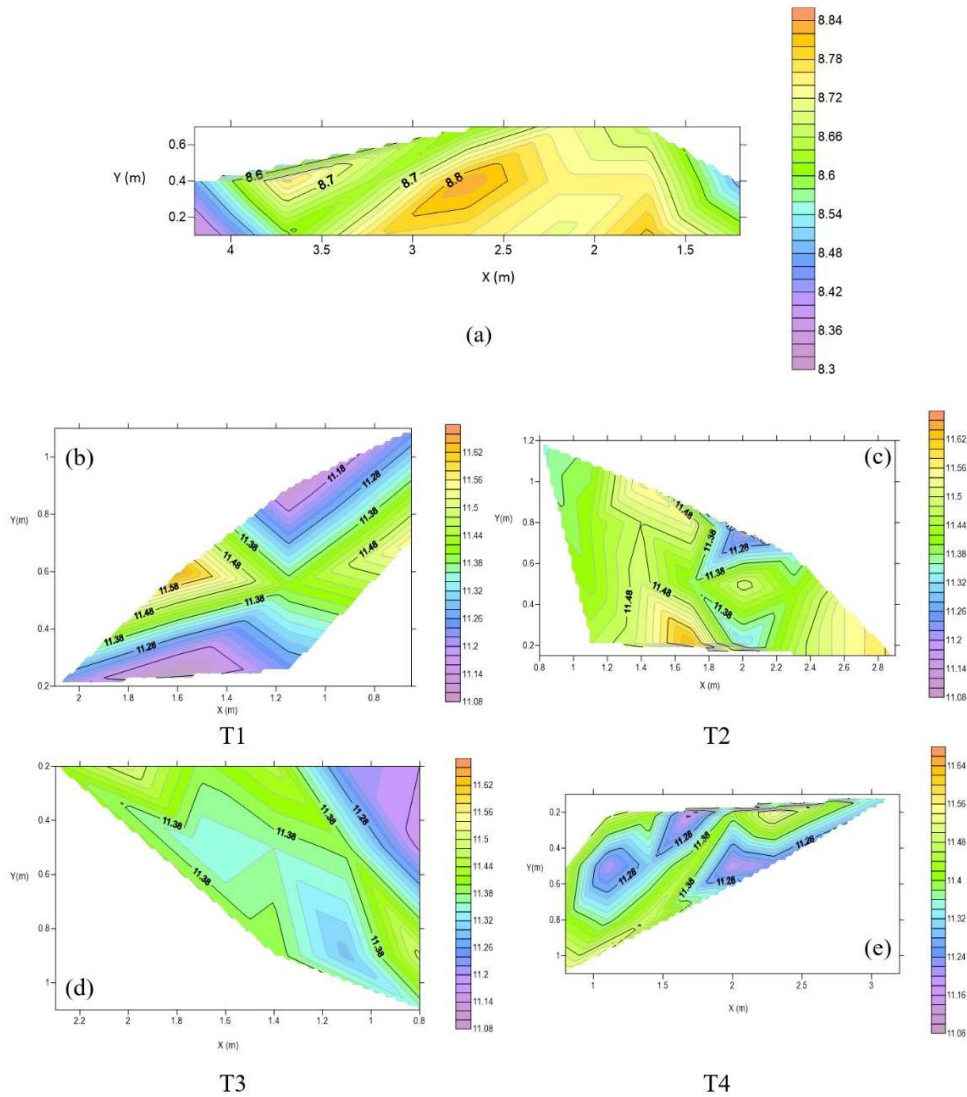


**Fig. 8:** Contour plot showing the distribution of pH in the untreated (a) and the cross-sections T1 (b), T2 (c), T3 (d), and T4 (e) of the lime-treated embankments measured during deconstruction

The pH measured from the specimens sampled at the upper layer (up to 0.12 m depth from the surface) of T1 and T2 was observed to be between 8.0 and 9.0 (Fig. 9). The trend of pH distribution in the upper layer of T1 and T2 appears to be almost similar.

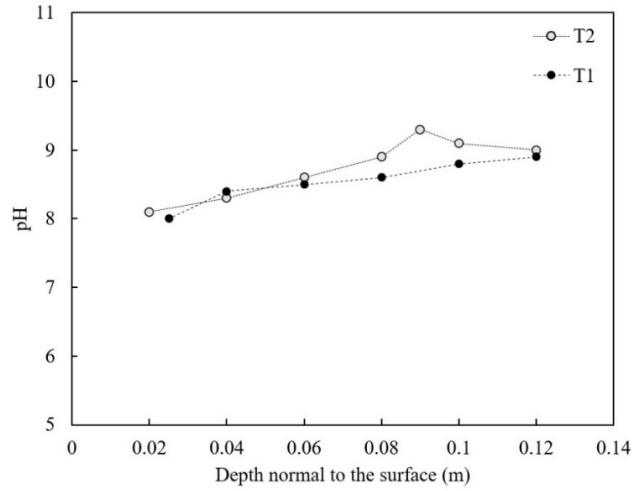


**Fig. 9:** pH measured on specimens sampled from the upper layer of the lime-treated embankment during deconstruction

#### 3.4. Pore size distributions

Fig. 10 (a-h) presents the PSD and cumulative pore volume of the untreated (Nat 1 and Nat 2) and the lime-treated specimens (T2-2 and T2-3) core-sampled at two different depths using MIP test and BJH method.

On investigating the pore structure of the untreated specimens by MIP, Nat 1 (0.15 m), and Nat 2 (0.45 m) a bimodal and unimodal PSD were observed, respectively (Fig. 10 (a)). Nat 1 shows the higher intensity of macropores diameter of around  $10^4$  and  $10^5$  Å, while Nat 2 shows the same around pore diameter  $10^4$  Å. The cumulative pore volume measured for Nat 1 was about 19 % higher than Nat 2 (Fig. 10 (b)). On observing the PSD and cumulative pore volume (in the range of pore diameter 20-250 Å) of the same untreated specimens by BJH, no significant presence of pores was observed in the mesopore range of pore diameter 50-500 Å (Fig. 10 (e & f)). Moreover, a similar narrow peak was seen at the pore diameter of 40 Å for both Nat 1 and Nat 2 (Fig. 10 (e)).

For the lime-treated specimens, the MIP results of both samples T2-2 (0.15 m) and T2-3 (0.45 m) show a broad unimodal peak at 625 Å with the development of smaller pores lower than pore diameter of 3000 Å (Fig. 10 (c)). The trend of PSD remains the same for T2-2 and T2-3. However, T2-2 shows 20 % lower total pore volumes than T2-3 (Fig. 10 (d)). While analysing the pore structure of these specimens by BJH, the trend of the PSD in the mesopore range of pore diameter 40-500 Å remains the same for both the lime-treated samples Fig. 10 (g). Both the specimens show a significant presence of mesopores of pore diameter in the range 50-500 Å. Specimen T2-2 shows a 27 % lower cumulative pore volume in the mesopore range of pore diameter 20-250 Å than T2-3 (Fig. 10 (h)). Additionally, a similar narrow peak at the pore diameter of 40 Å was observed for both T2-2 and T2-3 (Fig. 10 (g)).

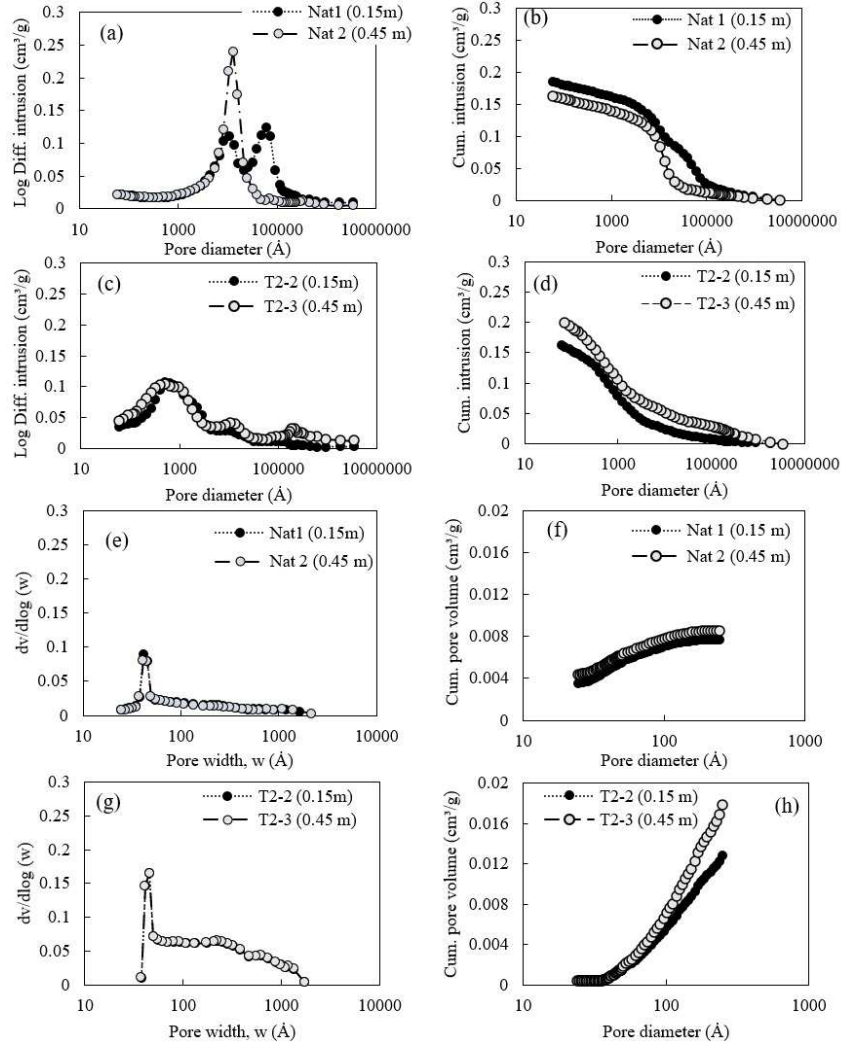
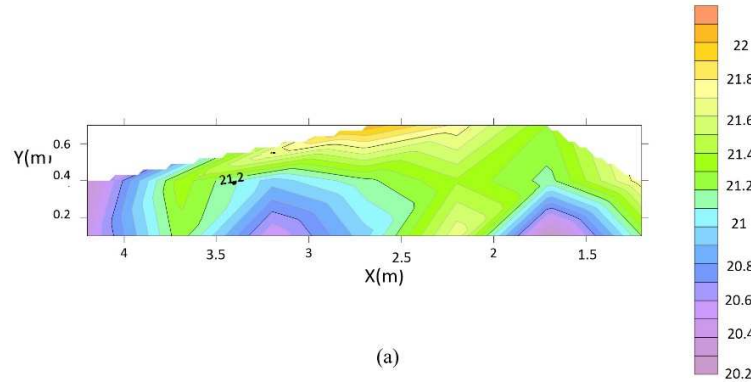


**Fig. 10:** PSD and Cumulative (Cum.) pore volume observed between untreated (Nat & Nat 2) and lime-treated specimens (T2-2 & T2-3) at a depth of 0.15 m & 0.45 m normal to the slope by MIP (a-d) & BJH (e-h) methods

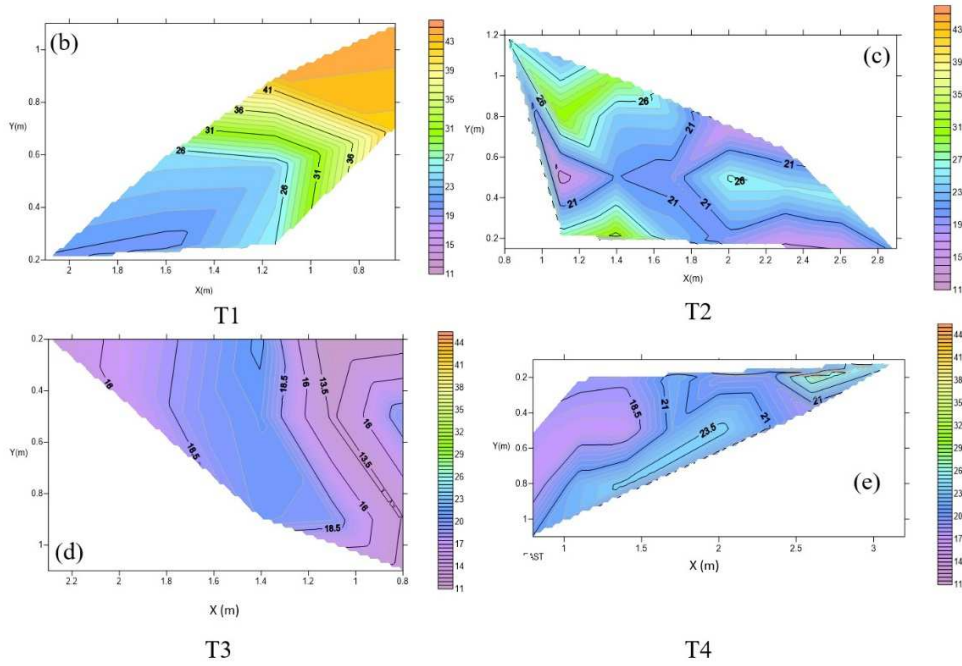
### 3.5. Distribution of SSA

Fig. 11 (a) shows the distribution of SSA throughout the core of the untreated embankment, which remains almost similar.

The SSA measured throughout the core of the lime-treated embankment appears to be unevenly distributed in all the cross-sections presented in Fig. 11 (b-e). The maximum range of SSA measured was between 40 m<sup>2</sup>/g and 45 m<sup>2</sup>/g, which was observed in few specimens sampled from T1 (Fig. 11 (b)), while other specimens show SSA values within 11 m<sup>2</sup>/g and 39 m<sup>2</sup>/g (Fig. 11 (b-e)).



(a)



**Fig. 11:** Contour plot showing the distribution of SSA ( $\text{m}^2/\text{g}$ ) in the untreated (a), and cross-sections T1 (b), T2 (c), T3 (d), and T4 (e) of the lime-treated embankments during deconstruction

## 4. Discussions

### 4.1. Evaluation of the UCS measured from the in-situ cured lime-treated specimens

Since specimens tested for the UCS had two different  $l/d$  ratios, a comparison between two samples of different ratios is made by applying a correction factor. According to ASTM-C42-77 (ASTM, 1978), a correction factor of 0.87 should be applied to the UCS measured using specimens with  $l/d = 1$  to obtain the corresponding UCS of a similar sample having  $l/d = 2$ . Thus, corrected UCS values of 4.35 ( $5.00 \times 0.87$ ) and 2.74 ( $3.16 \times 0.87$ ) MPa (Fig. 4) were obtained for T1-1 and T2-4, respectively. Expectedly, these corrected values are nearly equal to the UCS of specimens (T1-1 & T2-4) having  $l/d = 2$  (Fig. 4). Thus, considering different depths of sampling and different dimensions of the specimens, the UCS results can be assumed to be repeatable.

At the laboratory scale, the UCS measured from the accelerated cured specimen (Fig. 4) was corrected to 3.31 ( $3.80 \times 0.87$ ) MPa using the correction factor. The UCS of the in-situ specimens (Fig. 4) was observed to be about 2-4 times higher than what was measured after 28- and 90-days laboratory curing at 20°C. This highlights the contribution of lime treatment in increasing the UCS of the soil after long-term curing.

The average of the UCS value measured for the four in-situ cured specimens was  $3.29 (\pm 0.45)$  MPa. This average UCS value was found to be of comparable order to the UCS of the laboratory accelerated cured specimen of dimension having  $l/d = 2$  (3.31 MPa). This implies that such UCS levels can be expected after long-term curing. An inspection of the SEM images (Fig. 5 (b-d)) reveals that such evolution of UCS in the in-situ samples can be attributed to the formation of cementitious bonds as a result of pozzolanic reactions.

Another factor that can influence the in-situ measured UCS is the loss in water content. The water content measured in T1-1 and T2-4 during the UCS test was found to be 7 % lower than what was measured during the deconstruction period ( $\approx 18\%$ ) (Fig. 6 (b & c)). This loss of water occurred due to the complications faced at the time of the trimming of the block-sampled specimens in the laboratory, as mentioned in section 2.2. One might argue that this loss of water might have resulted in a higher UCS level than expected. However, the evolution of a comparable level of UCS in the laboratory accelerated cured specimens, the maintenance of pH greater than 11, and the formation of cementitious bonding support the fact that the observed level of UCS was unlikely to have been influenced by the loss of water.

#### 4.2. Contribution of mesopores generation towards strength evolution in lime-treated soil

The UCS of specimens T1-1 and T2-4 differs by 2 MPa (Fig. 4) even after they show similar water content during deconstruction ( $\approx 18\%$ ) and UCS test (11 %). Also, the pH measured during deconstruction was of the same level (Fig. 8 (b & c)). Thus, it can be derived that the observed difference in the UCS is not due to the difference in water content or pH. However, the suction measured for T1-1 corresponding to a water content of 17 % was 1.15 MPa, while it was 0.34 MPa for T2-4 at a water content of 16 % (Table 2). This difference in suction level might be due to differences in microstructural-development between T1-1 and T2-4 under the lime effect.

Lime treatment generates smaller pores (Cuisinier et al., 2011), which was shown to contribute to the rise in cohesion and hence strength (Verbrugge et al., 2011). In this aspect, the difference in smaller pores evolution between T1-1 and T2-4 was investigated by BJH method, as BJH method was observed to measure ranges of pores relatively lower than the one measured by MIP test in Fig. 10.

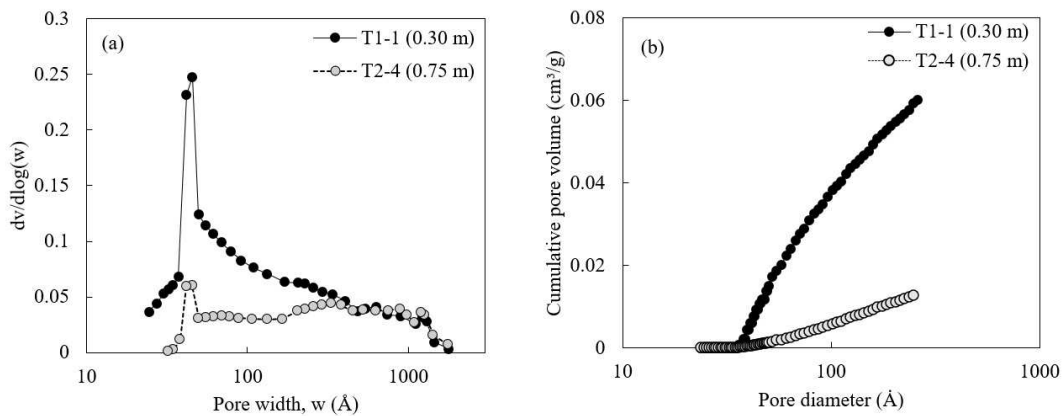


**Fig. 12:** Evolution of mesopores distribution (a) and cumulative pore volume (b) between T1-1 & T2-4 by BJH method

Fig. 12 shows the mesopores distribution of T1-1 and T2-4. In Fig. 12 (a), a narrow peak at a pore diameter of 40 Å was observed, which is five times higher in T1-1 than in T2-4. Moreover, a relatively large number of mesopores of pore diameter 50-500 Å was found in T1-1 compared to T2-4. Cumulatively, specimen T1-1 shows about 5.5 times higher presence of pore volume in the mesopores range of pore diameter 25-250 Å than T2-4 (Fig. 12 (b)).

Thus, this higher number of mesopores development in T1-1 has led to the increased suction and consequently resulted in greater strength in T1-1 than in T2-4.

#### *4.3. Long-term effect of lime treatment on the water content and pH distribution at the core of the embankments*

The average water content measured at the end of construction was 17.0 % and 19.4 % in the untreated and the lime-treated embankment, respectively. Thus, approximately a 5 % loss in water content was observed from the end of construction up to a depth of about 0.35 m normal to the surface of the untreated embankment (Fig. 6 (a)). This loss of water gradually decreases with depth. This was expected in the untreated embankment. The maximum loss of water in the core of the lime-treated embankment was about 2 % from the end of construction, comparatively lower than the untreated embankment.

Additionally, unlike the untreated embankment, the overall distribution of water content does not vary significantly with depth in the lime-treated embankment (Fig. 6 (b-e)). Most of the core-sampled specimens from the lime-treated embankment show water content ranging from 18.0 to 19.3 % (Fig. 6 (b-e)). Thus, this distribution can be said to be homogeneous. This can be attributed to the proper mixing and compaction process implemented during the construction time, as reported by Makki-Szymkiewicz et al. (2015). Thus, the presence of this homogeneous water content throughout the embankment and the lesser reduction in water content from the end of construction than the untreated embankment highlights the long-term water retention capacity of the lime-treated soil.

Lime treatment increases the pH of the natural soil due to the release of OH<sup>-</sup> ions in the soil-water-lime medium (Little, 1995). On evaluating the pH measured during deconstruction, the average pH measured in the untreated embankment was 8.5 (Fig. 8 (a)), which was found to be almost equivalent to the pH value of the present silty soil. However, all the lime-treated soil show pH greater than 11 (Fig. 8 (b-e)) and lower than 12.3, which corresponds to the pH at Lime Modification Optimum (LMO) of the soil. This decrease in pH can be attributed to the consumption of lime during the curing time, as demonstrated by De Bel et al. (2013). Besides, the difference measured in the pH level between the untreated and lime-treated soil evidences the presence of pozzolanic products within the core of the lime-treated embankment.

Like the homogenous distribution of water content observed throughout the core of the lime-treated embankment, the pH, too, was found to be uniformly distributed throughout, ranging from 11.08 to 11.66 (Fig. 8 (b-e)). This can also be attributed to proper mixing, as mentioned previously.

#### *4.4. Effect of lime treatment on the evolution of suction at the core of the embankments*

Within the range of suction measured for the untreated embankment (0.19 MPa-1.14 MPa), a total variation of around 1.00 MPa in suction corresponds to a 2 % (9.89 %-11.71 %) variation in water content (Table 2). At the same time, this variation is around 2.50 MPa (0.17 MPa-2.71 MPa) for the lime-treated soil corresponding to the same percentage difference in the water content (15.80 %-17.90 %). Thus, the maximum suction measured for the lime-treated soil was about 1.57 MPa higher than the untreated soil, although the corresponding water content in the lime-treated soil was about two times higher than the untreated soil. The average minimum suction measured for the untreated specimens approximately corresponds to the average maximum measured water content and vice versa (Table 2). This behaviour of suction variation with water content was expected in the untreated specimens. While in the lime-treated samples, the variation of suction was less affected by the difference in the water content level.

Makki-Szymkiewicz et al. (2015) reported a suction level of 0.051MPa to 0.084 MPa at about an average water content of 19.4 % in specimens collected up to 1 year from the end of construction in the same lime-treated embankment. Thus, the present measured suction range (0.17 MPa-2.71 MPa) in the lime-treated specimens increased by about 2 to 30 times with a maximum of 3 % difference in the level of water content (15.80-17.90 %) during the additional six years curing period. This can be attributed to the modification of the lime-treated soil microstructure illustrated by an additional generation of smaller pores ( $< 3000 \text{ \AA}$ ) (Fig. 10 (c)) in the present specimen compared to the MIP result reported by Makki-Szymkiewicz et al. (2015) for the six months in-situ cured specimen.

Besides, the present variation of suction with respect to water content (Table 2) was also compared with the water retention plot provided by Nguyen et al. (2015) for the same soil and are presented in Fig. 13. Nguyen et al. (2015) showed the evolution of suction with respect to volumetric water content for 28 days (28d) and 90 days (90d) laboratory cured specimens treated with 2 % and 4 % quicklime.

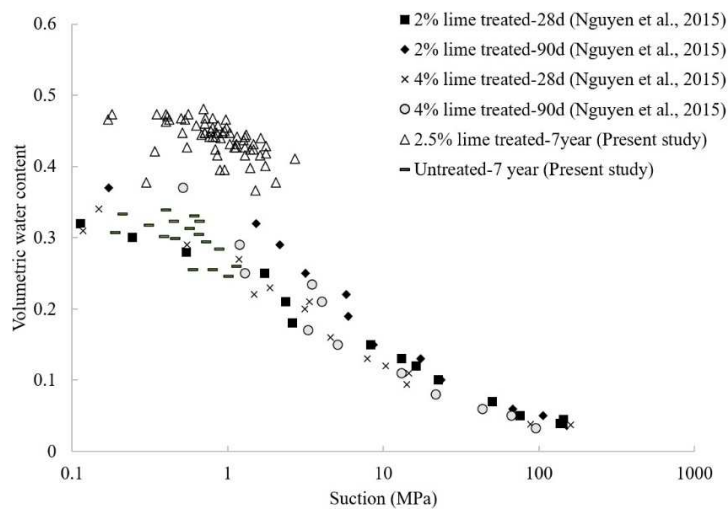


**Fig. 13:** Water retention plot obtained from the present soil compared to the one obtained from Nguyen et al. (2015)

Fig. 13 shows that the volumetric water content corresponding to the suction range of about 0.1 - 5.0 MPa was slightly higher for 90 days cured specimens compared to the corresponding 28 days cured specimens. Similar evolution of volumetric water content was observed in the present untreated soil corresponding to the suction range of 0.19-1.14 MPa. However, the volumetric water content in the 7-year cured specimens was about 50 % higher compared to all the specimens from Nguyen et al. (2015), corresponding to a similar range of suction (0.17-2.71 MPa).

Thus, based on the above discussion, it can be concluded that the observed long-term water retention capacity of the present lime-treated soil was due to this increased suction because of long-term pozzolanic reactions. Literature, based on laboratory studies, has demonstrated how lime treatment improves the water retention capacity of soil with the increase in curing time due to the modification of soil microstructure resulting from the generation of cementitious compounds (Russo, 2005; Wang et al., 2016).

Thus, the overall suction variation in the untreated soil follows the variation in the water content level inversely. However, in the lime-treated soil, the evolution of suction was due to the development of smaller pores as a result of pozzolanic reactions and was less affected by the variation in the water content level.

#### 4.5. Effectiveness of lime treatment on the upper layer of the embankment submitted to atmospheric exposure

The minimum water content measured in the upper-layer specimens of T1 and T2 was 7 % and 12 %, respectively (Fig. 7). This was about 12 % and 7 % less than the maximum water content measured in the core of T1 and T2, respectively (Fig. 6 (b & c)). The increase in loss of water as one moves from the core towards the upper layer emphasizes the effect of soil-atmosphere interaction. Besides, the development of vegetation roots (as observed during deconstruction) also contributes towards this water loss. Bicalho et al. (2018) and Rosone et al. (2018) reported a similar impact of soil-atmosphere interaction on the upper surface of an in-situ cured lime-treated embankment. They showed a significant loss of water from the surface to a depth of 0.45-0.75 m of the embankment. Thus, the present study shows that the influence of soil-atmosphere interaction is significant up to a depth of 0.12 m normal to the surface of the lime-treated embankment.

In addition to the loss of water, a maximum reduction in pH for T1 and T2 was observed to vary from 11.66 (Fig. 8 (b & c)) in the core to 8 in the upper layer (Fig. 9). This might be a consequence of carbonation (Xu et al., 2020) or dissolution of lime by leaching (Deneele et al., 2016; Khattab et al., 2007) under the long-term exposure of soil to the atmosphere. In the upper layer, the average pH for T1 and T2 gradually increases from around 8 near the surface to 9 corresponding to the depth of 0.12 m. This indicates that the atmospheric effects are minimised with depth.

Thus, it can be concluded that although the effect of lime treatment remains within the core of the lime-treated embankment, it was lost up to a depth of 0.12 m normal to the surface.

#### 4.6. Evaluation of pore structures measured between the untreated and the lime-treated soil

Unlike the MIP results of the untreated soil (Fig. 10 (a)), no significant macropores were found at a pore diameter of  $10^4$  Å and  $10^5$  Å in the lime-treated specimens (Fig. 10 (c)). Instead, both samples T2-2 and T2-3 show the presence of smaller pores of diameter lower than 3000 Å (Fig. 10 (c)). Such smaller pores formation due to lime treatment was also reported by Cuisinier et al. (2011). Additionally, in the lime-treated soil, as per the BJH results, the observed development of mesopores in the range of pore diameter 50 Å to 500 Å (Fig. 10 (g)) was more significant than that in the untreated soil (Fig. 10 (e)). The narrow peak developed at the pore width of 40 Å for the lime-treated specimens (Fig. 10 (g)) was about 1.8 times higher than what was observed in the untreated samples (Fig. 10 (e)). In the untreated specimens, this observed peak can be due to the presence of clay porosity (Bin et al., 2007; De Bel et al., 2013). The increase in this peak for the lime-treated samples might be due to the combined presence of clay porosity and cementitious bonding because of pozzolanic reactions.

The overall development of smaller pores in the lime-treated soil is attributed to the development of pozzolanic products (C-S-H, C-A-S-H, C-A-H, etc.), and not due to carbonation, as both T2-2 and T2-3 exhibit pH greater than 11 (Fig. 8 (c)), while carbonation reactions lead to a decrease in pH below 9 (Xu et al., 2020). Besides, the observed increase in smaller pores in the present 7-year cured specimens when compared to that reported by Makki-Szymkiewicz et al. (2015) (as explained in section 4.4) underscores the contribution of the pozzolanic reactions towards the development of smaller pores in the long-term.

Specimen Nat 1 (0.15 m) shows a higher number of macropores of pore width  $10^5$  Å and 19 % greater cumulative pore volume than Nat 2 (0.45 m), as reported in section 3.4. This indicates that the untreated specimen collected at a lower depth (0.15 m) exhibits more macropores than the one sampled from a greater depth (0.45 m). Samples Nat 1 and Nat 2 were located within the 2<sup>nd</sup> and the 3<sup>rd</sup> layer of compaction normal to the surface of the trench, respectively, in the untreated embankment (Fig. 2). Thus, during the construction of the untreated embankment, the compaction effort achieved by Nat 2 in the 3<sup>rd</sup> layer was higher than the one obtained by Nat 1 in the 2<sup>nd</sup> layer. Lipiec et al. (2012) and Mossadeghi-Björklund et al. (2019) have demonstrated how an increase in compaction effort leads to a decrease in the diameter of macropores with depths from the surface of the pavement. Thus, the presence of more macropores in Nat 1 than Nat 2 can be partly due to this difference in the compaction effort achieved with

respect to depth during construction. In the lime-treated embankment, specimen T2-2, located at 0.30 m above T2-3 (Fig. 3), shows a 27 % lower pore volume than T2-3 as per the BJH results (Fig. 10 (h)). However, specimen T1-1 located 0.45 m above T2-4, shows 5.5 times greater pores volume in the same pore range (Fig. 12 (b)).

Thus, it can be said that the presence of macropores in the untreated specimens are affected by the sampling-depth of the embankment, while the formation of mesopores in the lime-treated samples under the lime effect remains less affected by the same.

#### 4.7. Comparison between the volume of mesopores measured by MIP and BJH

The discussions in the preceding section show how lime treatment brings about the formation of pores smaller than 3000 Å in diameter, including mesopores. On comparing this formation of smaller pores detected using MIP (Fig. 10 (c)) and BJH (Fig. 10 (g)), it was observed that BJH results give a more precise distribution of intensities showing a narrow peak at 40 Å and a broad peak at 50-500 Å. This was missing in MIP results for the same specimens. Based on this observation, Table 3 is presented to show the percentage difference of cumulative pore volume in the mesopore range that can be accessed by both MIP and BJH methods. It includes specimens T2-2 and T2-3 in the pore range of mesopore diameter 60-250 Å (i.e., the intersection of the ranges accessible through MIP and BJH). Table 3 shows that the cumulative pore volume measured by BJH for T2-2 and T2-3, in the mesopore range (60-250 Å) was about 3.5 and 3.2 times higher than that measured by MIP, respectively.

**Table 3:**

Difference in pore volume measured in the mesopore range of pore diameter 60-250 Å by MIP and BJH methods

| Sample name   | Total $V_{cum}^1$<br>measured by<br>MIP<br>(60-3.5 × 10 <sup>6</sup> Å)<br>(cm <sup>3</sup> /g) | Total $V_{cum}$<br>measured by<br>BJH<br>(25-250 Å)<br>(cm <sup>3</sup> /g) | $V_{cum}$<br>measured by<br>MIP<br>(60-250 Å)<br>(cm <sup>3</sup> /g) | $V_{cum}$<br>measured by<br>BJH<br>(60-250 Å)<br>(cm <sup>3</sup> /g) | Calculated<br>$V_{cum}$<br>(60-250 Å)<br>as a percentage<br>of total measured<br>by MIP<br>(%) | Calculated<br>$V_{cum}$<br>(60-250 Å)<br>as a percentage<br>of total measured<br>by BJH<br>(%) |
|---------------|---|---|---|---|--|--|
| T2-2 (0.15 m) | 0.160   | 0.013   | 0.029   | 0.010   | 17.8   | 81.0   |
| T2-3 (0.45 m) | 0.200   | 0.018   | 0.040   | 0.015   | 19.8   | 84.0   |

<sup>1</sup> $V_{cum}$ : cumulative pore volume

These results, thus, show the effectiveness of the BJH method in quantifying the mesopores formed under long-term lime effect.

#### 4.8. Long-term effect of lime treatment on the SSA

Lime treatment is known to decrease the SSA of highly expansive soil based on laboratory investigations (Bhuvaneshwari et al., 2014; Cherian and Arnepalli, 2015). So far, the long-term effect of lime treatment on the SSA of lime-treated low plastic soil, such as silty soil, remains less investigated.

De Bel et al. (2013) conducted SSA by BET of the present MLD soil and stated that 3 % quick lime-treated MLD soil shows a decrease in SSA from 23.0 m<sup>2</sup>/g to 13.3 m<sup>2</sup>/g after 7 days of curing. At the same time, this SSA value rises to 21.6 m<sup>2</sup>/g after 400 days of curing at a laboratory scale. The former behaviour was attributed to the flocculation effect, while the latter to the formation of pozzolanic products (CSH and CAH). Considering this, it can be derived that the uneven distribution of SSA, as reported in Fig. 11 (b-e), could be linked to the development of cementitious compounds in the different specimens sampled at varying depths throughout the lime-treated embankment. As the evolution of cementitious

compounds leads to the formation of mesopores, the correlation between the range of mesopores generation and the evolution of SSA was evaluated by BJH.

Using BJH data, the percentage of cumulative pore volume present in the pore diameter range 25-250 Å was evaluated for specimens showing the maximum (T1-1 = 45 m<sup>2</sup>/g), the intermediate (T1-6 = 25 m<sup>2</sup>/g), and the minimum (T3-7 = 11 m<sup>2</sup>/g) SSA values. Fig. 14 (a) presents the percentage of pore volume for specimens over the range of pore diameter 25-250 Å at 25 Å intervals. It was observed that T1-1 shows about 11 % and 30 % higher pore volume in the range of pore diameter 25-75 Å than T1-6 and T3-7, respectively. T1-6 shows about 19 % higher pore volume in the same pore range than T3-7. For the remaining range of pore diameter (75-250 Å), the pore volume was observed to increase for T3-7, while it decreased more for T1-1 than T1-6. This indicates that the specimen with maximum SSA shows the presence of more pores of pore diameter 25-75 Å and vice versa.

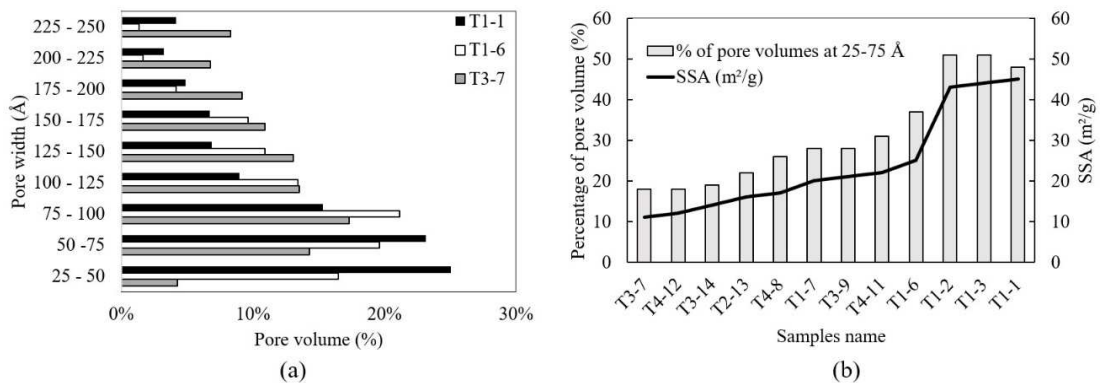


**Fig. 14:** Evolution of SSA with respect to the presence of pore volume in the mesopore range of pore diameter 25-75 Å

Based on this observation, the SSA of a few selected lime-treated specimens was plotted with respect to the evolution of pore volume in the range of pore diameter 25-75 Å (Fig. 14 (b)). An increase in the trend of pore volume was observed with the gradual rise in SSA. It can thus be derived that there exists an apparent correlation between the two quantities.

#### 4. Conclusions

The long-term effect of lime treatment on a silty soil embankment was evaluated in terms of mechanical, physicochemical, and microstructural properties after 7 years of atmospheric exposure in a wet climate. The evaluation was made by undergoing laboratory investigations using several specimens gathered in the upper layer as well as throughout the core of the embankment. Based on the study, the following conclusions are derived:

1. An average UCS level of 3.29 MPa was obtained from the in-situ cured lime-treated specimens. Comparison of this UCS level with the UCS obtained from the accelerated-cured sample (at 40°C after 90 days) at laboratory scale confirms that such UCS level can be expected from the in-situ cured specimens after 7 years of curing.
2. SEM images evidenced the presence of cementitious bonding formed because of pozzolanic reactions under the lime effect in the core-sampled specimens of the lime-treated embankment.
3. The lime effect persists throughout the core of the lime-treated embankment as the pH measurement was greater than 11 despite 7 years of curing in a region that receives significant rainfall throughout the year.

4. A maximum loss of 12 % and 18 % in the water content and pH, respectively, was observed in the upper layer-sampled specimens compared to the core-sampled specimens. This shows that the effect of lime was lost in the upper layer of the lime-treated embankment due to long-term exposure of the soil to the atmosphere and due to the development of vegetation roots.
5. The relevance of the combined MIP- and BJH-pore structure analysis is shown by their efficiency in representing the complete range of macropores and mesopores affected by lime-treatment. MIP highlights the reduction in macropores ( $10^4$ - $10^5$  Å) and an increase in the number of smaller pores ( $< 3000$  Å) in the lime-treated soil when compared to the untreated soil. Simultaneously, BJH shows the formation of mesopores (50-500 Å) in the lime-treated specimens, which was missing in the untreated soil. BJH method happens to define the evolution of mesopores under the lime effect more precisely than MIP.
6. The formation of smaller pores enhances the evolution of suction in the lime-treated core-sampled soil when compared to the untreated soil. This has led to a lower reduction in the water content during this 7-year curing period, and the distribution of water content remains less affected by depth. Thus, lime treatment improves the long-term water retention capacity of the soil.
7. The formation of mesopores in lime-treated specimens was less affected by the depth of sampling in the lime-treated embankment. These mesopores contribute to the evolution of strength and SSA. An increase in mesopores results in increased strength, while the SSA was found to be correlated to the presence of mesopores in the range of pore diameter 25-75 Å.

Thus, the study confirms the long-term persistence of the effect of lime within the core of a lime-treated silty soil embankment even after its exposure to a damp climate for 7 years. Based on the physicochemical and microstructural observations, a good and persistent mechanical performance was evidenced to be achieved at a lime content of 2.5 %.

## Acknowledgements

This work was financially supported by Association Nationale de la Recherche et de la Technologie with grant N°2018/0219 and Lhoist Southern Europe with grant N°RP2-E18114. The authors are very thankful to the research team of Université Gustave Eiffel, Lhoist Nivelles, and CEREMA Blois for their great support in performing field sampling, laboratory experiments, and technical support.

## References

- Akula, P., Hariharan, N., Little, D.N., Lesueur, D., Herrier, G., 2020. Evaluating the Long-Term Durability of Lime Treatment in Hydraulic Structures: Case Study on the Friant-Kern Canal. Transportation Research Record 0361198120919404. <https://doi.org/10.1177/0361198120919404>
- Ali, H., Mohamed, M., 2019. Assessment of lime treatment of expansive clays with different mineralogy at low and high temperatures. Construction and Building Materials 228, 116955. <https://doi.org/10.1016/j.conbuildmat.2019.116955>
- Al-Mukhtar, M., Khattab, S., Alcover, J.-F., 2012. Microstructure and geotechnical properties of lime-treated expansive clayey soil. Engineering geology 139, 17–27. <https://doi.org/10.1016/j.enggeo.2012.04.004>

- ASTM-C42-77., 1978. Standard method of obtaining and testing drilled cores and sawed beams of concrete. American Society for Testing and Materials, West Conshohocken, PA, USA.
- ASTM, D2166., 2006. Standard test method for unconfined compressive strength of cohesive soil. American Society for Testing and Materials, West Conshohocken, PA, USA.
- ASTM, D2216., 2010. Standard test methods for laboratory determination of water (moisture) content of soil and rock by mass. Annual Book of ASTM Standards.
- Aufmuth, R.E., 1970. Strength and Durability of Stabilized Layers under Existing Pavements. Army Construction Engineering Research Lab Champaign Ill.
- Barrett, E.P., Joyner, L.G., Halenda, P.P., 1951. The determination of pore volume and area distributions in porous substances. I. Computations from nitrogen isotherms. *Journal of the American Chemical society* 73, 373–380. <https://doi.org/10.1021/ja01145a126>
- Bell, F.G., 1996. Lime stabilization of clay minerals and soils. *Engineering geology* 42, 223–237. [https://doi.org/10.1016/0013-7952\(96\)00028-2](https://doi.org/10.1016/0013-7952(96)00028-2)
- Bhuvaneshwari, S., Robinson, R.G., Gandhi, S.R., 2014. Behaviour of lime treated cured expansive soil composites. *Indian Geotechnical Journal* 44, 278–293. <https://doi.org/10.1007/s40098-013-0081-3>
- Bicalho, K. v, Boussafir, Y., Cui, Y.-J., 2018. Performance of an instrumented embankment constructed with lime-treated silty clay during four-years in the Northeast of France. *Transportation Geotechnics* 17, 100–116. <https://doi.org/10.1016/j.trgeo.2018.09.009>
- Bin, S., Zhibin, L., Yi, C., Xiaoping, Z., 2007. Micropore structure of aggregates in treated soils. *Journal of materials in civil engineering* 19, 99–104. [https://doi.org/10.1061/\(ASCE\)0899-1561\(2007\)19:1\(99\)](https://doi.org/10.1061/(ASCE)0899-1561(2007)19:1(99))
- Brunauer, S., Emmett, P.H., Teller, E., 1938. Adsorption of gases in multimolecular layers. *Journal of the American chemical society* 60, 309–319. <https://doi.org/10.1021/ja01269a023>
- Cai, J., Hu, X., 2019. *Petrophysical Characterization and Fluids Transport in Unconventional Reservoirs*. Elsevier.
- Cardoso, R., das Neves, E.M., 2012. Hydro-mechanical characterization of lime-treated and untreated marls used in a motorway embankment. *Engineering geology* 133, 76–84. <https://doi.org/10.1016/j.enggeo.2012.02.014>
- Cherian, C., Arnepalli, D.N., 2015. A critical appraisal of the role of clay mineralogy in lime stabilization. *International Journal of Geosynthetics and Ground Engineering* 1, 8. <https://doi.org/10.1007/s40891-015-0009-3>
- Cui, H., Tang, W., Liu, W., Dong, Z., Xing, F., 2015. Experimental study on effects of CO<sub>2</sub> concentrations on concrete carbonation and diffusion mechanisms. *Construction and Building Materials* 93, 522–527. <https://doi.org/10.1016/j.conbuildmat.2015.06.007>
- Cuisinier, O., Auriol, J.-C., le Borgne, T., Deneele, D., 2011. Microstructure and hydraulic conductivity of a compacted lime-treated soil. *Engineering geology* 123, 187–193. <https://doi.org/10.1016/j.enggeo.2011.07.010>

729 De Bel, R., Gomes Correia, A., Duvigneaud, P. H., Francois, B., Herrier, G., Verbrugge, J. C., 2013.  
 730 Evolution mécanique et physico-chimique à long terme d'un sol limoneux traité à la chaux.  
 731 In Colloque Ter DOUEST.

732 Deneele, D., le Runigo, B., Cui, Y.-J., Cuisinier, O., Ferber, V., 2016. Experimental assessment regarding  
 733 leaching of lime-treated silt. *Construction and Building Materials* 112, 1032–1040.  
 734 <https://doi.org/10.1016/j.conbuildmat.2016.03.015>

735 Dhar, S., Hussain, M., 2019. The strength and microstructural behavior of lime stabilized subgrade soil in  
 736 road construction. *International Journal of Geotechnical Engineering* 1–13.  
 737 <https://doi.org/10.1080/19386362.2019.1598623>  
 738

739 di Sante, M., 2019. On the Compaction Characteristics of Soil-Lime Mixtures. *Geotechnical and*  
 740 *Geological Engineering* 1–10. <https://doi.org/10.1007/s10706-019-01110-w>  
 741

742 Diamond, S., Kinter, E.B., 1965. Mechanisms of soil-lime stabilization. *Highway Research Record* 92,  
 743 83–102.

744 Herrier, G., Chevalier, C., Froumentin, M., Cuisinier, O., Bonelli, S., Fry, J.-J., 2012. Lime treated soil as  
 745 an erosion-resistant material for hydraulic earthen structures.

746 Hopkins, T.C., Beckham, T.L., Sun, C., 2007. Stockpiling Hydrated Lime-Soil Mixtures.  
 747 <http://dx.doi.org/10.13023/KTC.RR.2007.12>

748 Jha, A.K., Sivapullaiah, P. v, 2019. Lime Stabilization of Soil: A Physico-Chemical and Micro-  
 749 Mechanistic Perspective. *Indian Geotechnical Journal* 1–9. [https://doi.org/10.1007/s40098-019-](https://doi.org/10.1007/s40098-019-00371-9)  
 750 00371-9  
 751

752 Khattab, S.A., Al-Mukhtar, M., Fleureau, J.-M., 2007. Long-term stability characteristics of a lime-treated  
 753 plastic soil. *Journal of materials in civil engineering* 19, 358–366.  
 754 [https://doi.org/10.1061/\(ASCE\)0899-1561\(2007\)19:4\(358\)](https://doi.org/10.1061/(ASCE)0899-1561(2007)19:4(358))

755 Knodel, P.C., 1987. Lime in canal and dam stabilization, US Bureau of Reclamation. Report No GR-87-  
 756 10, 21p.

757 Lemaire, K., Deneele, D., Bonnet, S., Legret, M., 2013. Effects of lime and cement treatment on the  
 758 physicochemical, microstructural and mechanical characteristics of a plastic silt. *Engineering*  
 759 *Geology* 166, 255–261. <https://doi.org/10.1016/j.enggeo.2013.09.012>

760 le Runigo, B., Cuisinier, O., Cui, Y.-J., Ferber, V., Deneele, D., 2009. Impact of initial state on the fabric  
 761 and permeability of a lime-treated silt under long-term leaching. *Canadian Geotechnical Journal* 46,  
 762 1243–1257. <https://doi.org/10.1139/T09-061>  
 763

764 Lipiec, J., Hajnos, M., Świeboda, R., 2012. Estimating effects of compaction on pore size distribution of  
 765 soil aggregates by mercury porosimeter. *Geoderma* 179, 20–27.  
 766 <https://doi.org/10.1016/j.geoderma.2012.02.014>

767 Little, D.N., 1995. Stabilization of pavement subgrades and base courses with lime.

768 Makki-Szymkiewicz, L., Hibouche, A., Taibi, S., Herrier, G., Lesueur, D., Fleureau, J.-M., 2015.  
 769 Evolution of the properties of lime-treated silty soil in a small experimental embankment.  
 770 *Engineering Geology* 191, 8–22. <https://doi.org/10.1016/j.enggeo.2015.03.008>

- Nguyen, T. T. H., Cui, Y. J., Herrier, G., Tang, A. M., 2015. Effect of lime treatment on the hydraulic conductivity of a silty soil. *Geotechnical Engineering for Infrastructure and Development*.
- McDonald, E.B., 1969. Lime Research Study, South Dakota Interstate Routes:(sixteen Projects). South Dakota Department of Highways, Materials and Soils Section.
- Mossadeghi-Björklund, M., Jarvis, N., Larsbo, M., Forkman, J., Keller, T., 2019. Effects of compaction on soil hydraulic properties, penetration resistance and water flow patterns at the soil profile scale. *Soil Use and Management* 35, 367–377. <https://doi.org/10.1111/sum.12481>
- Osula, D.O.A., 1996. A comparative evaluation of cement and lime modification of laterite. *Engineering geology* 42, 71–81. [https://doi.org/10.1016/0013-7952\(95\)00067-4](https://doi.org/10.1016/0013-7952(95)00067-4)
- Rosone, M., Ferrari, A., Celauro, C., 2018. On the hydro-mechanical behaviour of a lime-treated embankment during wetting and drying cycles. *Geomechanics for Energy and the Environment* 14, 48–60. <https://doi.org/10.1016/j.gete.2017.11.001>
- Rouquerol, J., D. Avnir, C. W. Fairbridge, D. H. Everett, J. M. Haynes, N. Pernicone, J. D. F. Ramsay, K. S. W. Sing, K. K. Unger., 1994. Recommendations for the characterization of porous solids (Technical Report). *Pure and Applied Chemistry* 66, no. 8: 1739-1758.
- Russo, G., 2005. Water retention curves of lime stabilised soil. *Advanced experimental unsaturated soil mechanics* 391–396.
- Verbrugge, J.-C., de Bel, R., Correia, A.G., Duvigneaud, P.-H., Herrier, G., 2011. Strength and micro observations on a lime treated silty soil, in: *Road Materials and New Innovations in Pavement Engineering*. pp. 89–96. [https://doi.org/10.1061/47634\(413\)12](https://doi.org/10.1061/47634(413)12)
- Wang, Y., Cui, Y.-J., Tang, A.M., Benahmed, N., 2016. Aggregate size effect on the water retention properties of a lime-treated compacted silt during curing, in: *E3S Web of Conferences*. EDP Sciences, p. 11013. <https://doi.org/10.1051/e3sconf/20160911013>
- Webb, P.A., Orr, C., 1997. Analytical methods in fine particle technology. Micromeritics Instrument Corp.
- Xu, L., Zha, F., Liu, C., Kang, B., Liu, J., Yu, C., 2020. Experimental Investigation on Carbonation Behavior in Lime-Stabilized Expansive Soil. *Advances in Civil Engineering*. <https://doi.org/10.1155/2020/7865469>
- Zhang, Y., Daniels, J.L., Cetin, B., Baucom, I.K., 2020. Effect of Temperature on pH, Conductivity, and Strength of Lime-Stabilized Soil. *Journal of Materials in Civil Engineering* 32, 04019380. [https://doi.org/10.1061/\(ASCE\)MT.1943-5533.0003062](https://doi.org/10.1061/(ASCE)MT.1943-5533.0003062)